

Phase-field modeling of nonlinear material behavior

Y.-P. Pellegrini, C. Denoual and L. Truskinovsky

Abstract Materials that undergo internal transformations are usually described in solid mechanics by multi-well energy functions that account for both elastic and transformational behavior. In order to separate the two effects, physicists use instead phase-field-type theories where conventional linear elastic strain is quadratically coupled to an additional field that describes the evolution of the reference state and solely accounts for nonlinearity. In this paper we propose a systematic method allowing one to split the non-convex energy into harmonic and nonharmonic parts and to convert a nonconvex mechanical problem into a partially linearized phase-field problem. The main ideas are illustrated using the simplest framework of the Peierls-Nabarro dislocation model.

1 Introduction

Non-convex energy potentials are used in solid mechanics for the modeling of martensitic transformations [8], plasticity [1] and fracture [23]. Parts of the resulting energy landscapes correspond to sufficiently smooth deformations preserving the locally affine structure of the lattice environment of each atom. Other parts represent highly distorted atomic arrangements associated with either loss or reacquisition of nearest neighbors. While deformations of the first type can (often) be described by

Y.-P. Pellegrini and C. Denoual
CEA, DAM, DIF, F-91297 Arpajon, France,
e-mail: yves-patrick.pellegrini@cea.fr, christophe.denoual@cea.fr

L. Truskinovsky
Laboratoire de Mécanique des Solides, CNRS UMR-7649, École Polytechnique, Route de Saclay,
F-91128 Palaiseau Cedex, France, e-mail: trusk@lms.polytechnique.fr

Paper submitted to: K. Hackl (ed.), *Proceedings of the IUTAM Symposium on Variational Concepts with Applications to the Mechanics of Materials, September 22-26, 2008, Bochum* (Springer-Verlag), to appear.

the conventional strain tensor of (linear) elasticity theory, a representation of the deformations of the second type requires introducing additional internal variables accounting for deviations from the local affinity of the stressed atomic configurations. In particular, these supplementary variables describe the evolution of the local reference state (LRS) from which the elastic deformations are measured [2, 10, 24]. The main difference between the elastic strains and these supplementary internal variables is that the dynamics of the former is typically inertial, while that of the latter is usually overdamped.

The coarse-grained non-convex energy density $f(\varepsilon)$ is usually known either from extrapolations of experimental measurements or from *ab-initio* calculations involving atomic homogeneity constraints. We assume that the argument ε of this function, that represents a coarse-grained strain, is small and can be additively split into the linear elastic part e , and a phase-field part η that accounts for the nonlinear evolution of the LRS. Our second assumption is that f can be represented as a sum of two terms: the elastic energy f_e , which depends on $e = \varepsilon - \eta$ and the phase-field energy g , which depends on η . We interpret $f(\varepsilon)$ as the outcome of adiabatic elimination of the variable η and consider the inverse problem of recovering the phase-field energy $g(\eta)$ from the function $f(\varepsilon)$ under the assumption that the function $f_e(e)$ is quadratic. The problem of the identification of $g(\eta)$ reduces to a problem of optimization and the relation between the 'optimally' related functions $f(\varepsilon)$ and $g(\eta)$ is studied in some prototypical cases. If, in contrast, the function $g(\eta)$ is chosen arbitrarily, the corresponding function $f(\varepsilon)$ is typically non-smooth and non single-valued, e.g. [5].

To motivate the need for the phase-field variables we consider in full detail a specific physical example. It deals with the mixed, discrete-continuum representation of a dislocation core [11, 15]. More specifically, we develop a modified version of the classical Peierls-Nabarro (PN) model that accounts for a finite thickness of the slip region. In this problem the coarse-grained description of the slip zone is provided by the so-called γ -potential [4, 25]. The phase field represents an "atomically sharp" slip and the part of the interaction potential related to g gives rise to the slip-related pull-back force [6, 15, 22]. Our general method of recovering the expression for this force represents an extension of Rice's transform, which was first introduced in the context of a dislocation nucleation problem [18].

In this paper only the simplest scalar problem in a one-dimensional setting is considered. The slightly more general question of extracting from the coarse-grained energy a convex (instead of quadratic) component will be examined elsewhere [16].

2 Surface problem

We begin with the special case when the phase field is localized on a surface. In problems involving fracture or slip it often proves convenient to represent the energy of a body as the sum of a bulk term depending on strain gradients and a surface term penalizing displacement discontinuities. The bulk term is usually modeled by

linear elasticity. The modeling of the surface energy is less straightforward [5, 23]. For instance, the models will be different depending on whether the location of the discontinuities is known a priori or not.

In a 1D setting with a known fracture set the equilibrium problem reduces to minimizing the following energy functional

$$W[u] = \int_0^1 dx f_e(u_x) + \sum_{\Gamma_a} f_a(\delta(x)). \quad (1)$$

Here $f_e(e) = (E/2)e^2$, $E > 0$ is the elastic modulus and a is a coarse-graining length scale that typically exceeds several atomic sizes. The set Γ_a in (1) represents discontinuity points resolved at scale a and $\delta(x) = [u]_a(x)$ is the corresponding displacement discontinuity. The surface energy $f_a(\delta)$ is then an effective interaction over the distance a ; in particular, the shear-related component of $f_a(\delta)$ coincides the γ -potential mentioned in the Introduction.

In the case when the fracture set is unknown the surface energy has to be chosen differently. Observe, for instance, that the displacement discontinuity at scale a does not represent the microscopic slip between neighboring atomic planes, and therefore the difference between elastic deformation and inelastic slip has not been resolved [18]. More precisely, linear elasticity, which has nothing to do with slip and which is already accounted for in the bulk term, has not been excluded from $f_a(\delta)$. The identification of the surface energy in (1) with $f_a(\delta)$, which is quadratic at the origin, leads in a free discontinuity problem to a degenerate solution with infinitely many infinitely small discontinuities [5].

To remove linear elasticity from the surface term, one should replace the coarse-grained discontinuity $[u]_a$ by the atomically sharp slip $\eta(x) = [u](x)$ that does not depend on a . The energy (1) is then rewritten as

$$W[u] = \int_0^1 dx f_e(u_x) + \sum_{\Gamma} g(\eta), \quad (2)$$

where now Γ is the set of discontinuity points corresponding to $a = 0$. The problem is to find the relation between the function $f_a(\delta)$, representing an empirical input, and the unknown function $g(\eta)$.

To define $g(\eta)$ we divide the total slip δ into an elastic part, ae , where e is an equivalent elastic strain, and an inelastic part η . The function $g(\eta)$ is defined by the condition that $f_a(\delta)$ is a relaxation of the energy $af_e(e) + g(\eta)$ under the condition that $ae + \eta = \delta$, namely:

$$f_a(\delta) = \inf_{\eta, \text{loc.}} \left[a \frac{E}{2} \left(\frac{\delta - \eta}{a} \right)^2 + g(\eta) \right]. \quad (3)$$

Our task is to reverse this definition and to recover the nonequilibrium energy $g(\eta)$ from $f_a(\delta)$. What allows us to proceed is the specific (harmonic) structure of the elastic part of the energy.

Recall that the function g must satisfy the following necessary condition

$$\frac{E}{a}(\delta - \eta) = g'(\eta), \quad (4)$$

which can also be written as

$$f'_a(\delta) = \frac{E}{a}(\delta - \eta). \quad (5)$$

These two equations allow one to represent $g'(\eta)$ in the following parametric form [6, 7, 18]

$$(\eta, g'(\eta)) = \left(\delta - \frac{a}{E} f'_a(\delta), f'_a(\delta) \right). \quad (6)$$

The parametric representation for $g(\eta)$ then reads

$$(\eta, g(\eta)) = \left(\delta - \frac{a}{E} f'_a(\delta), f_a(\delta) - \frac{a}{2E} [f'_a(\delta)]^2 \right). \quad (7)$$

Since for nonconvex $f_a(\delta)$ this representation may lead to a multivalued function $g(\eta)$ formula (7) must be supplemented by an additional branch selection procedure. To illustrate the mapping $f(\delta) \rightarrow g(\eta)$ given by (7) and the selection of a

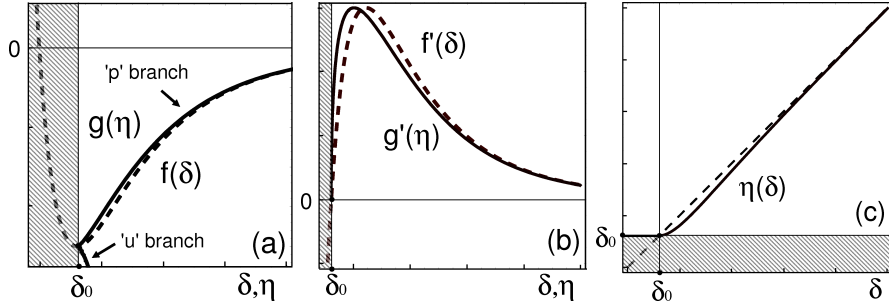


Fig. 1 Parametric transforms (6), (7) applied to a Lennard-Jones potential $f(\delta) = \delta^{-12} - \delta^{-6}$. a) $f(\delta)$ (dashed), and the two branches of $g(\eta)$ (solid), where 'p' ('u') labels the physical (unphysical) branch; b) $f'(\delta)$ and the 'p' branch of $g'(\eta)$; c) $\eta(\delta)$.

physical branch we consider a Lennard-Jones potential f_a , with $a = 1$ and assume that $E = f''(\delta_0)$, where δ_0 is the only minimum of f (see Fig. 1). Notice that the resulting function $g'(\eta)$ has an infinite slope at $\eta = \delta_0$ and that for $\eta \gtrsim \delta_0$ we must have $g(\eta) \propto (\eta - \delta_0)^{3/2}$.

The removal of the linear elastic part of the energy becomes important in PN-type modeling of dislocations. Consider, for instance, a straight screw dislocation in an isotropic linear-elastic body and assume that the sharp discontinuity plane, $y = 0$, lies between the two effective gliding surfaces located at $y = \pm a/2$. To account for the finite thickness of the core region a we need to modify the classical PN

model [11]. According to our interpretation the linear elastic stress outside the slip region $(-a/2, a/2)$ must be balanced by the coarse-grained pull-back stress that is resolved at the spatial scale a . We therefore interpret the pull-back stress at this scale as $f'_a(\delta(x))$, where f_a is the γ -potential, a periodic function with period b and with $f'_a(0) = 0$. The expression for the linear stress outside the slip region is derived in the Appendix.

With these considerations in mind we obtain for the unknown function $\eta(x)$ representing a mathematical slip at $y = 0$ the following system of equations

$$-\frac{\mu}{\pi a} \int_{-\infty}^{+\infty} dx' \eta'(x') \arctan \frac{a}{2(x-x')} + \bar{\sigma}_a(x) = f'_a(\delta(x)), \quad (8)$$

$$\delta(x) = \frac{a}{\mu} f'_a(\delta(x)) + \eta(x), \quad (9)$$

where $\bar{\sigma}_a$ is the resolved applied stress at scale a . If we match the linear elastic behavior at $\eta = 0$ with that in the bulk regions we obtain that $\mu = a f''_a(0)$. Using in this relation the physical shear modulus and the value of $f''_a(0)$ from the γ -potential provides a rough estimate for a , the effective interaction range.

We notice that parameter a enters both equations (8,9), which makes this system different from the one studied in [15, 18]. The ideas behind our nonlocal extension of the PN model are also different from that of Ref. [12] where a non-local kernel was introduced empirically as part of the pull-back stress, and the regular $1/(x-x')$ kernel was used for the bulk stress.

To bring the system (8,9) into the framework of phase-field models, we identify the effective pull-back force $f'_a(\delta(\eta))$ with $g'(\eta)$ and rewrite Eq. (8) as

$$\frac{\mu}{2} \int_{-\infty}^{+\infty} dx' K_a(x-x') \eta'(x') + \bar{\sigma}_a(x) = g'(\eta). \quad (10)$$

where $K_a(x) = -(2/\pi a) \arctan(a/2x)$. It is now easy to see that $g'(\eta)$ enjoys the parametric representation

$$(\eta, g'(\eta)) = \left(\delta - \frac{a}{\mu} f'_a(\delta), f'_a(\delta) \right), \quad (11)$$

where we recognize the mapping (6) (see also [18, 22, 15]). To make the link with the classical PN model one needs to consider the limit $a \rightarrow 0$. By computing η in terms of δ and expanding (10) in powers of a , we obtain to order $O(a)$ the following 'gradient' extension of the PN model

$$-\frac{\mu}{2\pi} \int_{-\infty}^{+\infty} dx' \frac{\delta'(x')}{x-x'} + \lambda \delta''(x) + \tilde{\sigma}_a(x) = f(\delta(x)), \quad (12)$$

where $\lambda = a\mu/4$. For different weakly or strongly nonlocal generalizations of the PN model see [12, 20]. Equation (12) features an effective applied stress that differs from $\sigma_a(x, 0)$ defined in the Appendix by an $O(a)$ correction, namely $\tilde{\sigma}_a(x) \equiv$

$\sigma_a(x, 0) + (a/2) [(1/2)\partial_y \sigma_a(x, 0) - K_0 \star \partial_x \sigma_a(x, 0)]$. The classical PN model is retrieved by letting $a = 0$.

3 Bulk problem

Now let us place the problem in a more general framework. The task is to approximate locally the empirical potential $f(\varepsilon)$ by a quadratic function with an optimally chosen reference state η , and to associate with this state a reference energy $g(\eta)$. Behind such construction is the assumption that all the nonlinearity of the problem is related to the evolution of the reference state. The simplest setting to pose formally the problem is the one dimensional geometrically linearized theory of nonlinear elastic bars.

According to our interpretation the empirical energy is represented as

$$f(\varepsilon) = \inf_{\eta, \text{loc.}} \left[\frac{E}{2} (\varepsilon - \eta)^2 + g(\eta) \right] \quad (13)$$

and the problem is to find the intrinsic phase-field function $g(\eta)$. Following the previous section we write the parametric representation for $g'(\eta)$ in the form

$$(\eta, g'(\eta)) = \left(\varepsilon - \frac{f'(\varepsilon)}{E}, f'(\varepsilon) \right). \quad (14)$$

The function $g(\eta)$ is then given by the mapping

$$(\eta, g(\eta)) = \left(\varepsilon - \frac{f'(\varepsilon)}{E}, f(\varepsilon) - \frac{f'(\varepsilon)^2}{2E} \right). \quad (15)$$

The consistency of this procedure requires the parameter E and the function $f(\varepsilon)$ to be related. If we expand the parametric definition of $g(\eta)$ near a reference state ε_0 where $f'(\varepsilon_0) = 0$, we obtain $g(\varepsilon_0) = f(\varepsilon_0)$, $g'(\varepsilon_0) = 0$ and $g''(\varepsilon_0) = f''(\varepsilon_0)/[1 - f''(\varepsilon_0)/E]$. The natural choice $E = f''(\varepsilon_0)$ makes $g''(\varepsilon_0)$ infinite. The behavior of the higher derivatives of $g(\eta)$ near $\eta = \varepsilon_0$ is found by assuming (without loss of generality) that derivatives $f^{(k)}(\varepsilon_0)$ vanish for $k = 3, \dots, n-1$. The order of the asymptotics depends on $n > 2$, which is the first integer such that $f^{(n)}(\varepsilon_0) \neq 0$:

$$(\eta, g(\eta)) \simeq \left(\varepsilon_0 - \frac{f^{(n)}(\varepsilon_0)}{(n-1)!E} \delta \varepsilon^{(n-1)}, f(\varepsilon) - \frac{(n-1)f^{(n)}(\varepsilon_0)}{n!} \delta \varepsilon^n \right). \quad (16)$$

Hence g behaves near its minimum as: $|g(\eta) - g(\varepsilon_0)| \sim |\eta - \varepsilon_0|^{\frac{n}{n-1}}$. The generic case is $n = 3$; the case $n = 4$ corresponds to periodic potential relevant for dislocations; for f locally harmonic, $n = \infty$.

Observe now that the function g computed from (14,15), can also be viewed as a solution of the following optimization problem:

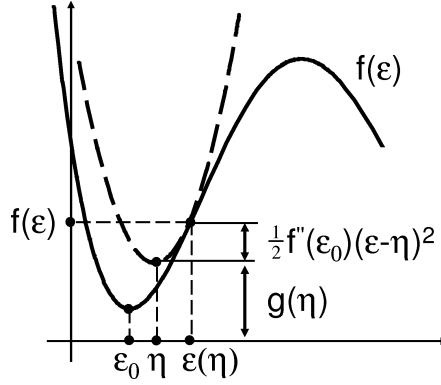


Fig. 2 Geometrical illustration of the construction defined by Eqs. (14-17).

$$g(\eta) = \sup_{\varepsilon, \text{loc.}} \left[f(\varepsilon) - \frac{E}{2}(\varepsilon - \eta)^2 \right], \quad (17)$$

which is a natural inverse of (13) (see also [17, 19]). Since the equation $\eta = \varepsilon - f'(\varepsilon)/E$ may have several solutions $\varepsilon(\eta)$, the representation (17) removes the ambiguity by always selecting the upper branch.

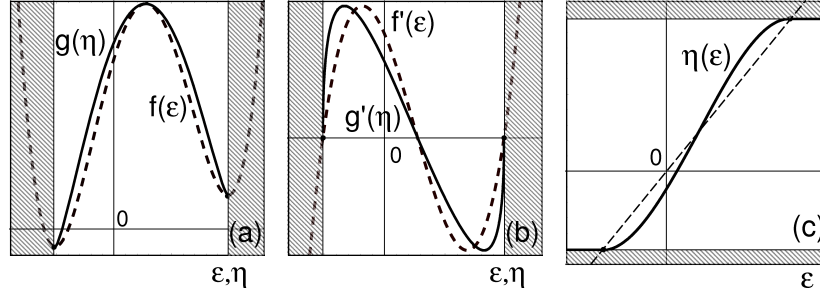


Fig. 3 Phase-field representation of a double-well potential $f(\varepsilon) = (\varepsilon - 1)^2(2\varepsilon + 1)^2 + 0.2\varepsilon$.

The working of Eqs. (14-17) with $E = f''(\varepsilon_0)$ is illustrated in Fig. 2. In the domain at the left of ε_0 , where f grows faster than harmonic the desired tangency point does not exist. In this case the difference $f(\varepsilon) - \frac{E}{2}(\varepsilon - \eta)^2$ is maximized at $\varepsilon = -\infty$. This situation takes place in the Lennard-Jones example of Sec. 2 where we have to use $g(\delta) = +\infty$ for $\delta < \delta_0$ (hatched area of Fig. 1a).

To handle multi-well energies, we first introduce the Stillinger-Weber mapping $\varepsilon_0(\varepsilon)$ that links to any state ε the local minimum ε_0 of $f(\varepsilon)$ that would be attained from this state by steepest-descent [21]. Next, we modify equations (13) and (17) as:

$$f(\varepsilon) = \inf_{\eta, \text{loc}} \left[\frac{1}{2} f''(\varepsilon_0(\varepsilon)) (\varepsilon - \eta)^2 + g(\eta) \right], \quad (18)$$

$$g(\eta) = \sup_{\varepsilon, \text{loc}} \left[f(\varepsilon) - \frac{1}{2} f''(\varepsilon_0(\eta)) (\varepsilon - \eta)^2 \right]. \quad (19)$$

Whereas (19) defines g , equation (18) states that knowing f is equivalent to knowing g plus the linear-elastic behavior of f near its local minima.

The precise meaning of the “loc” in Eqs. (18), (19) is as follows. Operationally, the minimization in the definition of f is carried out over η , starting from $\varepsilon_0(\varepsilon)$, the local minimum nearest to ε determined by the SW mapping; the corresponding elastic modulus is also determined by the starting point. The maximization in the definition of $g(\eta)$ proceeds along similar lines except that now the relevant elastic modulus is determined by the local minimum closest to η , and is fixed during the maximization. The optimization is carried out starting from $\varepsilon = \eta$.

Figs. 3 illustrate the case of a double-well potential with unequal curvatures of the wells. Notice that in contrast to what we saw in Fig. 1 the function $\eta(\varepsilon)$ is now bounded.

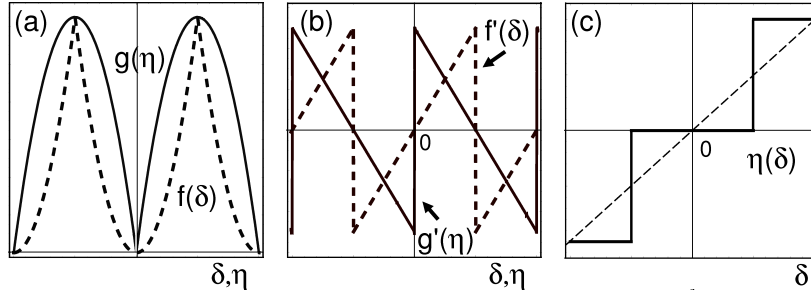


Fig. 4 Transform (19) applied to the piecewise-harmonic periodic potential $f(\delta) = (\delta - [\delta])^2/2$. Notation $[\cdot]$ stands for the integer part. The function $\eta(\delta)$ is determined as the argmin in (18).

Another interesting case is the periodic potential that is used in the description of reconstructive phase transitions (e.g., [3]). Consider, for instance, the piecewise-harmonic *periodic* case shown in Fig. 4 that is often used in analytical studies [12, 20]. The parametric representation (14) of g is here useless and the definition (19) must be used instead. In this extreme case, *all* elasticity has been removed from g and the resulting $g(\eta)$ is cone-shaped at its minima (Fig. 4a) as predicted by Eq. (16) for $n \rightarrow \infty$. The force $g(\eta)$ is discontinuous (Fig. 4b) and its extreme values provide thresholds for the evolution of η , whose stepwise character is an artifact due to the absence of smooth spinodal regions in f .

It is also instructive to consider for comparison the case of an unbounded harmonic potential $f(\varepsilon) = (E_f/2)(\varepsilon - \varepsilon_0)^2$. From (17) with $E = E_f$, one deduces that $g(\eta) = +\infty$ if $\eta \neq \varepsilon_0$ and $g(\eta = \varepsilon_0) = 0$. This trivial example indicates that in a purely linear-elastic model, the reference state does not have to evolve.

References

1. Carpio, A., Bonilla, L.L.: Discrete models for dislocations and their motion in cubic crystals. *Phys. Rev. B* **12**, 1087–1097 (2005)
2. Choksi, R., Del Piero, G., Fonseca, I., Owen, D.R.: Structural deformations as energy minimizers in models of fracture and hysteresis. *Math. Mech. Solids* **4**, 321–356 (1999)
3. Conti, S., Zanzotto, G.: A variational model for reconstructive phase transformations, and their relation to dislocations and plasticity. *Arch. Rational Mech. Anal.*, **173**, 69–88 (2004)
4. Christian, J.W., Vitek, V.: Dislocations and stacking faults. *Rep. Prog. Phys.* **33**, 307–411 (1970)
5. Del Piero, G., Truskinovsky L.: Macro and micro-cracking in 1D elasticity. *Int. J. Solids Struct.* **38**, 1135–1148 (2001)
6. Denoual, C.: Dynamic dislocation modeling by combining Peierls-Nabarro and Galerkin methods. *Phys. Rev. B* **70**, 024106 (2004)
7. Denoual, C.: Modeling dislocations by coupling Peierls-Nabarro and element-free Galerkin methods. *Comput. Meth. Appl. Mech. Engrg.* **196**, 1915–1923 (2007)
8. Ericksen, J.: Equilibrium of bars. *J. Elast.* **5**, 191–202 (1975)
9. Eshelby, J.D.: Uniformly moving dislocations. *Proc. Phys. Soc. London A* **62**, 307–314 (1949)
10. Hakim, V., Karma, A.: Crack path prediction in anisotropic brittle materials. *Phys. Rev. Lett.* **95**, 235501 (2005)
11. Hirth, J.P., Lothe J.: *Theory of dislocations* (2nd edn.). Wiley & Sons, New York (1982)
12. Miller, R., Phillips, R., Beltz, G., Ortiz, M.: A non-local formulation of the Peierls dislocation model. *J. Mech. Phys. Solids* **46**, 1845–1867 (1998)
13. Mura, T.: *Micromechanics of defects in solids* (2nd edn.). Martinus Nijhof, Dordrecht (1987).
14. Nabarro, F.R.N.: Dislocations in a simple cubic lattice. *Proc. Phys. Soc.* **59**, 256–272 (1947)
15. Ortiz, M., Phillips, R.: Nanomechanics of defects in solids. *Adv. Appl. Mech.* **36**, 1–79 (1999)
16. Pellegrini, Y.-P., Denoual C., Truskinovsky, L., in preparation.
17. Ponte Castañeda, P., Suquet, P.: Nonlinear composites. *Adv. Appl. Mech.* **34**, 171–302 (2002)
18. Rice, J.R.: Dislocation nucleation from a crack tip: an analysis based on the Peierls concept. *J. Mech. Phys. Solids* **40**, 239–271 (1992)
19. Rockafellar, T.: *Convex analysis*. Princeton University Press, Princeton (1997)
20. Rosakis, P.: Supersonic dislocation from an augmented Peierls model. *Phys. Rev. Lett.* **86**, 95–95 (2001)
21. Stillinger, F.H., Weber, T.A.: Packing structures and transitions in liquids and solids. *Science* **225**, 983–989 (1984)
22. Sun, Y., Beltz, G.E., Rice, J.R.: Estimates from atomic models of tension-shear coupling in dislocation nucleation from a crack tip. *Mat. Sci. Eng. A* **170**, 69–85 (1993)
23. Truskinovsky, L.: Fracture as a phase transformation. In: Batra, R. and Beatty, M. (eds.) *Contemporary research in mechanics and mathematics of materials*, pp. 322–332. CIMNE, Barcelona (1996)
24. Wang, Y., Khachaturyan, A.G.: Three-dimensional field model and computer modeling of martensitic transformations. *Acta Mater.* **45**, 759–773 (1997)
25. Woodward, C.: First-principles simulations of dislocation cores, *Mat. Sci. Engrg. A* **400-401**, 59–67 (2005)

4 Appendix

The following computations are largely based on the Eshelby’s arguments presented in [9]. Consider a Volterra dislocation with zero-width core and with Burgers vector b . The displacement $u_z(x, y)$ has the form

$$u_z(x, y) = b \frac{\text{Arg}(x + iy)}{2\pi} = \frac{b}{2\pi} \arctan \frac{y}{x} + \frac{b}{2} \text{sign}(y) \theta(-x), \quad (20)$$

where θ is the Heaviside function, and where the indeterminacy in the discontinuity of u_z is resolved by specifying both the glide plane ($y = 0$) and the past history of the dislocation (our dislocation “came” from $x = -\infty$).

The distributional part in the r.h.s. of Eq. (20), usually omitted in the literature (e.g. [11]), is crucial to the present derivation because it represents the memory of the irreversible atomic displacements on the plane $y = 0$. We introduce the eigendistortion [13], β_{ij}^* , as the part of the dislocation-induced distortion $\beta_{ij} = u_{i,j}$, that is *not* linear-elastic. For our dislocation, its only non-zero component is $\beta_{yz}^*(x, y) = b \theta(-x) \delta_D(y)$, where δ_D is the Dirac distribution. The displacement is obtained as a convolution of β^* with the Green function G_{ij} . In Fourier space $\beta_{yz}^*(k_x, k_y) = b \pi \delta_D(k_x) + i b / k_x$ and we can write

$$u_z(x, y) = -i \int \frac{dk_x dk_y}{(2\pi)^2} G_{3k}(k_x, k_y, k_z = 0) k_l C_{klmn} \beta_{nm}^*(k_x, k_y) e^{i(k_x x + k_y y)}$$

where C_{ijkl} is the elastic tensor. For an isotropic medium,

$$C_{ijkl} = \mu \left(\frac{2\nu}{1-2\nu} \delta_{ij} \delta_{kl} + \delta_{ik} \delta_{jl} + \delta_{il} \delta_{jk} \right),$$

$$G_{ij}(\mathbf{k}) = \frac{1}{\mu k^2} \left[\delta_{ij} - \frac{k_i k_j}{2(1-\nu)k^2} \right],$$

where μ is the shear modulus and ν is the Poisson ratio. Thus,

$$u_z(x, y) = -i \int \frac{dk_x dk_y}{(2\pi)^2} \frac{k_y}{k_x^2 + k_y^2} \beta_{yz}^*(k_x, k_y) e^{i(k_x x + k_y y)}.$$

The r.h.s. of (20) follows provided that care is exercised with respect to the distributional parts in the singular Fourier integral (a principal value is implicit in the definition of $\beta_{yz}^*(k_x, k_y)$).

The linear elastic distortion, β_{ij}^e , is defined through the additive decomposition of the total distortion β_{ij} , namely $\beta_{ij}^e \equiv \beta_{ij} - \beta_{ij}^*$ [13]. The elastic strains are $e_{ij} = \text{sym} \beta_{ij}^e$. By using the identity $[\arctan(1/x)]' = \pi \delta_D(x) - 1/(1+x^2)$, we obtain that the distributional parts in β_{ij} and β_{ij}^* mutually cancel out giving the standard result [11]

$$e_{xz}(x, y) = -\frac{b}{4\pi} \frac{y}{x^2 + y^2}, \quad e_{yz}(x, y) = \frac{b}{4\pi} \frac{x}{x^2 + y^2}. \quad (21)$$

The stress induced by the eigenstrain is then $\sigma_{iz}^*(x, y) = 2\mu e_{iz}(x, y)$, where $i = x, y$.

In the presence of an applied shear stress [14] $\sigma_a \equiv \sigma_{ayz}$, Eq. (20) becomes

$$u_z(x, y) = \frac{1}{\mu} \int_0^y dy' \sigma_a(x, y') + \frac{b}{2\pi} \arctan \frac{y}{x} + \frac{b}{2} \text{sign}(y) \theta(-x), \quad (22)$$

The total stress is then $\sigma = \sigma^* + \sigma_a$ and $e = \sigma/2\mu$. Now, the key step consists in averaging the stress over the layer of width a containing the glide plane. Introduce:

$$\overline{\sigma}_{ij}(x) \equiv \frac{1}{a} \int_{-a/2}^{+a/2} dy \sigma_{ij}(x, y).$$

From (22), the x component of the total relative atomic lattice displacement between the atomic planes at $y = \pm a/2$ reads:

$$\delta(x) \equiv u_z(x, +a/2) - u_z(x, -a/2) = \frac{a}{\mu} \left[\overline{\sigma}_a(x) + \frac{\mu b}{\pi a} \arctan\left(\frac{a}{2x}\right) \right] + b \theta(-x). \quad (23)$$

Furthermore on account of (21) the average shear stress $\overline{\sigma}_{yz}(x)$ in the layer is:

$$\overline{\sigma}_{yz}(x) = \overline{\sigma}_a(x) + \frac{\mu b}{2\pi} \frac{1}{a} \int_{-a/2}^{+a/2} dy \frac{x}{x^2 + y^2} = \overline{\sigma}_a(x) + \frac{\mu b}{\pi a} \arctan\left(\frac{a}{2x}\right). \quad (24)$$

Comparison of (24) and (23) shows that:

$$\delta(x) = \frac{a}{\mu} \overline{\sigma}_{yz}(x) + b \theta(-x). \quad (25)$$

Consider next an Eshelby screw dislocation with an extended core described by a continuous function $\eta(x)$. The distortion β^* becomes:

$$\beta_{yz}^*(x, y) = \delta_D(y) \eta(x) = -\delta_D(y) \int_x^{+\infty} dx' \eta'(x'). \quad (26)$$

The above Volterra dislocation corresponds to the limiting case $\eta(x) = b \theta(-x)$. Displacements, strains and stresses are obtained by convolution using $d\beta_{yz}^*(x, y) \equiv -\delta_D(y) \eta'(x) dx$ [9] as elementary distortions. The analogs of Eqs. (24,25) are:

$$\overline{\sigma}_{yz}(x) = \overline{\sigma}_a(x) - \frac{\mu}{\pi a} \int_{-\infty}^{+\infty} dx' \arctan\left(\frac{a}{2(x-x')}\right) \eta'(x') \quad (27)$$

$$\delta(x) = \frac{a}{\mu} \overline{\sigma}_{yz}(x) + \eta(x). \quad (28)$$

Equation (28), which we use in the paper, shows the relation between the coarse-grained displacement δ , and the discontinuity η .